

## Comparative study of the photoresponse from tetracene-based and pentacene-based thin-film transistors

Jeong-M. Choi, Jiyoul Lee, D. K. Hwang, Jae Hoon Kim, and Seongil Im<sup>a)</sup>  
*Institute of Physics and Applied Physics, Yonsei University, Seoul 120-749, Korea*

Eugene Kim

*Department of Information Display Engineering, Hongik University, Seoul 121-791, Korea*

(Received 15 June 2005; accepted 6 December 2005; published online 26 January 2006)

We report on the photoresponse from tetracene-based and pentacene-based thin-film transistors (TFTs) with semitransparent NiO<sub>x</sub> source/drain electrodes and SiO<sub>2</sub>/p<sup>+</sup>-Si substrate. Both organic TFTs have been fabricated with identical channel thickness and device geometry. Compared with pentacene-based TFTs, the tetracene-TFT exhibited superior potentials as a photodetector in the visible and ultraviolet range although it showed a field mobility ( $\mu=0.003$  cm<sup>2</sup>/V s) which is two orders of magnitude lower than that of the pentacene-based TFT ( $\mu\sim 0.3$  cm<sup>2</sup>/V s). The tetracene-TFT displayed a high photo-to-dark current ratio ( $I_{ph}/I_{dark}$ ) of  $3\times 10^3$ , while that of the pentacene-TFT was only  $\sim 10$ . © 2006 American Institute of Physics. [DOI: 10.1063/1.2168493]

Pentacene-based thin-film transistors (TFTs) have been extensively studied so far because their device performance characteristics almost surpass amorphous Si-based TFTs in terms of field-effect mobility and also because they can be fabricated even at room temperature (RT).<sup>1-4</sup> The low-temperature processing has even led to the realization of a transparent flexible substrate coated with a transparent polymer gate dielectric/electrode for TFT fabrication.<sup>5-8</sup> However, pentacene-based photonic devices have rarely been reported although the energy gap for solid pentacene is known to be about 1.9 eV.<sup>9,10</sup>

Tetracene, which is another important organic molecule composed of four benzene rings, has been known to be inferior to pentacene in terms of electronic transport performance in its solid forms.<sup>11</sup> Its optical energy gap for the highest occupied molecular orbital-lowest unoccupied molecular orbital (HOMO-LUMO) is known to be  $\sim 2.3$  eV (Refs. 12 and 13) and tetracene-based light-emitting TFT for much high voltage action ( $\sim 80$  V) has been reported very recently.<sup>14,15</sup> Although no photodetecting properties in a practical format has been reported for a tetracene yet, it is expected that solid tetracene probably has distinct advantages for a photonic device as well as for a light emitter.

For device applications of an organic molecular crystal, it is important to check their photoelectric properties, i.e., whether they are photosensitive or not. Photoinsensitive crystals may serve as good electronic device components overcoming the interference of ambient light while highly sensitive ones should be employed as an active layer of a photodetecting device. In the present study, we have fabricated both tetracene and pentacene-based TFTs with semitransparent NiO<sub>x</sub> source/drain (S/D) electrodes to investigate the photosensitivities of these two important organic TFTs, in which the semitransparent electrode guarantees effective photoabsorption in the whole area of our organic TFT channels.

A substrate of 200 nm thick SiO<sub>2</sub> on p<sup>+</sup>-Si ( $\sim 0.01$  Ω cm) was prepared for the gate dielectric and elec-

trode of our TFTs. Tetracene and pentacene channel layers of 50 nm thickness were then patterned on the substrates at RT by thermal evaporation at an identical deposition rate of 0.1 nm/s. These organic films were confirmed to be crystalline as measured by x-ray diffractometry (using Cu K<sub>α</sub> x ray) but the crystallinity of the tetracene films appeared somewhat inferior to that of pentacene. Subsequently, 100 nm thick NiO<sub>x</sub> was evaporated onto the pentacene and tetracene channels through a S/D mask at RT. For this S/D evaporation, we have used NiO powder (99.97%) in a tungsten crucible. The effectiveness of the NiO<sub>x</sub> electrode was previously reported elsewhere.<sup>16</sup> The NiO<sub>x</sub> layer was also deposited on Corning glass 7059 for separate optical transmittance and sheet resistance measurements. The transmittance was about 30% in the visible and the sheet resistance was 100 Ω/□. Finally, we applied In paste onto the back side of p<sup>+</sup>-Si for a large-area ohmic contact. The nominal channel length and width of our TFT were 90 μm and 500 μm, respectively. The inset of Fig. 1 shows a schematic cross section of our organic phototransistor.

All electrical and photoelectric characterizations were carried out with a semiconductor parameter analyzer (Model

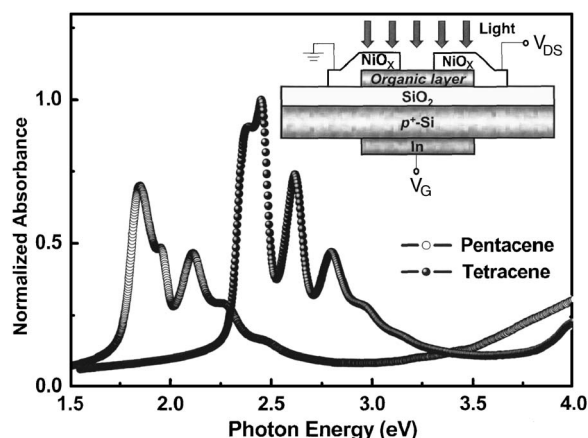


FIG. 1. Absorption spectra of thermally evaporated 100 nm thick tetracene and pentacene films deposited on Corning glass 7059. The inset shows a schematic cross section of our organic TFTs.

<sup>a)</sup> Author to whom correspondence should be addressed; electronic mail: semicon@yonsei.ac.kr

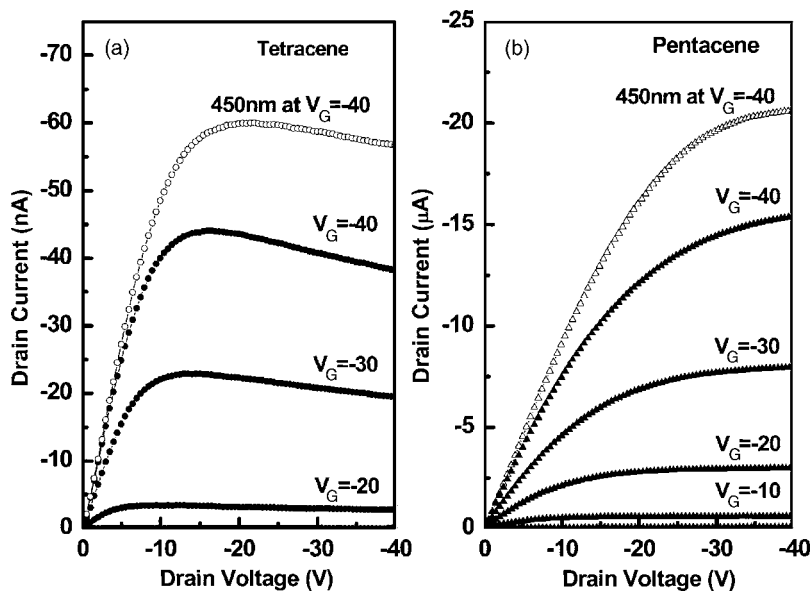


FIG. 2.  $I_D$ - $V_D$  curves obtained from (a) our  $\text{NiO}_x/\text{tetracene}$ - and (b)  $\text{NiO}_x/\text{pentacene}$ -based TFT in the dark and with the blue illumination (450 nm).

HP 4155C, Agilent Technologies) at RT. Light illumination was performed on our TFT setup, as shown in the inset of Fig. 1, with a light source (Oriental Optical System) consisting of a 500 W Hg (Xe) arc lamp and a monochromator covering the wavelength in the range of 350–700 nm. The optical power of the incident monochromatic light was measured by an ultraviolet (UV)-enhanced Si detector (Advantest TQ 8210) and in the present study the optical power density of all illuminations [630 nm (red), 540 nm (green), 450 nm (blue)] was fixed to  $\sim 0.1 \text{ mW/cm}^2$ . Absorption measurements were performed with a Varian Cary 5G Spectrophotometer on the both organic films with 100 nm thickness that had been deposited on Corning glass at the same deposition rate of 0.1 nm/s.

Figure 1 displays the normalized absorbance spectra obtained from 100 nm thick tetracene and pentacene films deposited on Corning glass. Optical energy gaps were 2.3 and 1.85 eV for tetracene and pentacene films, respectively, and their absorption spectra were similar to previously reported ones.<sup>9,17</sup> The absorbance of tetracene appeared relatively higher than that of pentacene with the identical thickness. This means that solid tetracene more effectively absorbs the photons with energies over its optical energy gap (2.3 eV) than solid pentacene.

The drain current-drain voltage ( $I_D$ - $V_D$ ) characteristics of tetracene-based and pentacene-based TFTs are shown in Figs. 2(a) and 2(b), respectively. The saturation current obtained from a pentacene-TFT was two orders of magnitude higher than that from a tetracene-TFT while both organic TFTs showed some amount of photocurrent under a blue light of 450 nm. At the same gate bias ( $V_G$ ) of  $-40 \text{ V}$ , their drain current increased by 35–50% under the illumination. These demonstrate their initial potentials for photodetecting devices. However, differences in their capacities appear in Fig. 3. According to the  $\sqrt{-I_D}$ - $V_G$  plots of pentacene- and tetracene-TFTs, pentacene-TFT reveals its excellence as a carrier transporter with a high-field mobility ( $\mu$ ) of  $0.3 \text{ cm}^2/\text{V s}$  while the tetracene-TFT's mobility is limited to  $0.003 \text{ cm}^2/\text{V s}$ . Despite the inferior mobility, the tetracene-TFT can be turned on by the blue light at much lower gate voltage, responding well to the light. Under the blue light, the threshold voltage ( $V_T$ ) of the tetracene-TFT was very

much shifted from its initial position (in the dark) to the positive-voltage side by more than 16 V (see the arrows of Fig. 3). This light-induced  $V_T$  shift was only about 6 V for the pentacene-TFT (inset).

These differences in the photoresponse between the two organic TFTs were exhibited in  $\log_{10}(-I_D)$ - $V_G$  curves of Fig. 4(a) in a more detailed manner. As shown in the inset of Fig. 4(a), our pentacene-TFT showed little photoelectric effects throughout the visible range with energies over the pentacene optical gap (1.85 eV, 670 nm) even in the depletion regime of gate bias [see the arrow at  $+16 \text{ V}$  in the inset of Fig. 4(a)]. On the other hand, the tetracene-TFT displayed relatively large photocurrent under visible to UV illuminations except for the red light, of which the photon energy is lower than the HOMO-LUMO gap of solid tetracene (see Fig. 1). Besides, the photoresponse of our tetracene device under red light appears still better than that of our pentacene device. It is likely that some mid-gap states exist within the HOMO-LUMO gap of our solid tetracene films and thus that some carriers trapped in the mid-gap states respond to red illumination. Our tetracene-TFT also displayed some optical power dependence for its photoresponse. With an increased UV power of  $0.64 \text{ mW/cm}^2$ , the device exhibited enhanced pho-

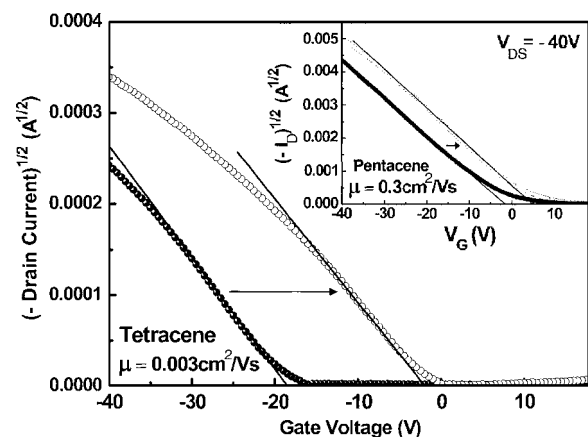


FIG. 3.  $\sqrt{-I_D}$ - $V_G$  curves obtained from our  $\text{NiO}_x/\text{tetracene}$ -based TFT. The inset shows  $\sqrt{-I_D}$ - $V_G$  curves taken from our  $\text{NiO}_x/\text{pentacene}$ -based TFT.

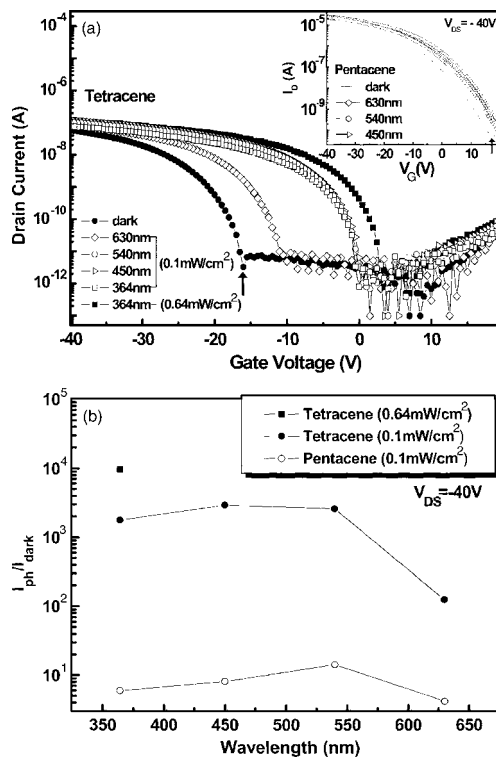


FIG. 4. (a)  $\log_{10}(-I_D) - V_G$  curves obtained at a  $V_{DS} (= -40$  V) from the both of our  $\text{NiO}_x/\text{tetracene}$ - and  $\text{NiO}_x/\text{pentacene}$ -based TFTs, illuminated by visible and UV lights. (b) Photo-to-dark current ratio ( $I_{ph}/I_{dark}$ ) for tetracene and pentacene-based TFTs as a function of the illumination wavelength in a depletion regime with a minimum drain current [see the arrows in (a)].

to current although the current increase was actually not very high.

The photo-to-dark current ratio ( $I_{ph}/I_{dark}$ ) for tetracene and pentacene-based TFTs was plotted with the wavelength of light in Fig. 4(b), where the  $I_{dark}$  was taken to be the minimum current at the depletion regime as indicated by the arrows in Fig. 4(a). The tetracene-based TFT displayed two orders of magnitude higher  $I_{ph}/I_{dark}$  ratio than that of the pentacene-based device. In the depletion regime, the tetracene-TFT showed higher photocurrent ( $\sim 30$  nA) than the pentacene case ( $\sim 1$  nA) even in terms of the absolute current level. It is worth understanding why the tetracene-TFT exhibits more pronounced photoelectric effects even in the absolute current level. Taking some important hints from the case of organic photovoltaic cells, we may speculate the following points. For the photocurrent gain of the cells, it is necessary to consider four general processes: Photoabsorption (exciton generation), exciton diffusion to an electrode, dissociation of the excitons, the drift of the dissociated free carriers to the electrode. The exciton binding energy in tetracene crystals is inferred to be somewhat larger than that in pentacene crystals.<sup>13</sup> Moreover, the drift mobility in the solid tetracene was two orders of magnitude lower than that in solid pentacene, as shown in Fig. 3. In spite of those disadvantages, however, our tetracene-TFT displayed much higher photoelectric performances than the pentacene-TFT: two orders of magnitude higher  $I_{ph}/I_{dark}$  ratio [Fig. 4(b)] and much larger turn-on voltage shift (Fig. 3). It is initially because the photoabsorption (or the photogenerated exciton density) of the tetracene film was superior to that of the pentacene film with identical thickness as observed in Fig. 1, but more primarily because the exciton diffusion length or exciton life

time in solid tetracene is much longer than that in solid pentacene.<sup>18–20</sup> According to the literature, the exciton life time in solid tetracene ( $\sim 200$  ps) is two orders of magnitude longer than that in solid pentacene ( $\sim 1$  ps)<sup>18–20</sup> and thus our photoelectric results from tetracene-based TFTs are now quite understandable.

In summary, we have demonstrated the photosensitivity of the two important organic TFTs: Tetracene- and pentacene-based thin-film transistors on  $\text{SiO}_2/p^+-\text{Si}$  substrates with semitransparent  $\text{NiO}_x$  S/D electrodes. The tetracene-TFT exhibited excellent potentials as a photodetector in the visible and UV range showing effective photoabsorption and considerable light-induced shift of turn-on voltage although the device also displayed two orders of magnitude lower-field mobility ( $\mu = 0.003$   $\text{cm}^2/\text{V s}$ ) than the pentacene-based TFT ( $\mu = \sim 0.3$   $\text{cm}^2/\text{V s}$ ). The tetracene-TFT displayed a high photo-to-dark current ratio ( $I_{ph}/I_{dark}$ ) of  $3 \times 10^3$  while the pentacene-TFT showed the corresponding ratio of only  $\sim 10$ . We thus conclude that our tetracene-TFT is highly promising as an effective photodetector.

The authors are very appreciative of the financial support from KISTEP (Program No. M1-0214-00-0228) and KRF (Program No. C00047), and they also acknowledge the support from Brain Korea 21 Program. One of the authors (J. H. K.) acknowledges financial support from Yonsei University Research (Fund No. 1999-1-0029) and eSSC at Postech funded by MOST through KOSEF.

- <sup>1</sup>R. A. Street, D. Knipp, and A. R. Völkel, *Appl. Phys. Lett.* **80**, 1658 (2002).
- <sup>2</sup>H. Klauk, D. J. Gundlach, M. Bonse, C. C. Kuo, and T. N. Jackson, *Appl. Phys. Lett.* **76**, 1692 (2002).
- <sup>3</sup>D. Knipp, R. A. Street, A. Völkel, and J. Ho, *J. Appl. Phys.* **93**, 347 (2003).
- <sup>4</sup>D. J. Gundlach, Y. Y. Lin, T. N. Jackson, S. F. Nelson, and D. G. Schlom, *IEEE Electron Device Lett.* **18**, 87 (1997).
- <sup>5</sup>F. Eder, H. Klauk, M. Halik, U. Zschieschang, G. Schmid, and C. Dehm, *Appl. Phys. Lett.* **84**, 2673 (2004).
- <sup>6</sup>H. Klauk, M. Halik, U. Zschieschang, F. Eder, G. Schmid, and C. Dehm, *Appl. Phys. Lett.* **82**, 4175 (2003).
- <sup>7</sup>M. Halik, H. Klauk, U. Zschieschang, T. Kriem, G. Schmid, W. Radlik, and K. Wussow, *Appl. Phys. Lett.* **81**, 289 (2002).
- <sup>8</sup>M. Halik, H. Klauk, U. Zschieschang, G. Schmid, W. Radlik, and W. Weber, *Adv. Mater. (Weinheim, Ger.)* **14**, 1717 (2002).
- <sup>9</sup>S. S. Kim, Y. S. Choi, K. Kim, J. H. Kim, and S. Im, *Appl. Phys. Lett.* **82**, 639 (2003).
- <sup>10</sup>J. Lee, S. S. Kim, K. Kim, J. H. Kim, and S. Im, *Appl. Phys. Lett.* **84**, 1701 (2004).
- <sup>11</sup>D. J. Gundlach, J. A. Nichols, L. Zhou, and T. N. Jackson, *Appl. Phys. Lett.* **80**, 2925 (2002).
- <sup>12</sup>M. Pope, and C. E. Swenberg, *Electronic Processes in Organic Crystals and Polymers*, 2nd ed. (Oxford University Press, New York, 1999).
- <sup>13</sup>K. Hummer and C. Ambrosch-Draxl, *Phys. Rev. B* **71**, 081202(R) (2005).
- <sup>14</sup>A. Hepp, H. Heil, W. Weise, M. Ahles, R. Schmechel, and H. V. Seggern, *Phys. Rev. Lett.* **91**, 157406 (2003).
- <sup>15</sup>C. Santato, I. Manunza, A. Bonfiglio, F. Cicoira, P. Cosseddu, R. Zamboni, and M. Muccini, *Appl. Phys. Lett.* **86**, 141106 (2005).
- <sup>16</sup>J. M. Choi, D. K. Hwang, J. H. Kim, and S. Im, *Appl. Phys. Lett.* **86**, 123505 (2005).
- <sup>17</sup>A. K. Ghosh and T. Feng, *J. Appl. Phys.* **44**, 2781 (1973).
- <sup>18</sup>V. K. Thorsmølle, R. D. Averitt, X. Chi, D. J. Hilton, D. L. Smith, A. P. Ramirez, and A. J. Taylor, *Appl. Phys. Lett.* **84**, 891 (2004).
- <sup>19</sup>S. V. Frolov, Ch. Kloc, J. H. Schön, and B. Batlogg, *Chem. Phys. Lett.* **334**, 65 (2001).
- <sup>20</sup>V. K. Thorsmølle, R. D. Averitt, J. Demsar, X. Chi, S. Tretiak, A. P. Ramirez, and A. J. Taylor, in *Trends in Optics and Photonics*, edited by A. A. Sawchuk (Optical Society of America, Washington, DC, 2004), Vol. 97, pp. 441 and 442.